Scientific paper

Synthesis and Characterization of Alkylammonium Zwitterionic Amino Acids Derivatives by FTIR, NMR Spectroscopy and DFT Calculations

Iwona Kowalczyk

Laboratory of Microbiocides Chemistry, Faculty of Chemistry, Adam Mickiewicz University, Grunwaldzka 6, 60-780 Poznań, Poland,

** Corresponding author: E-mail: iwkow@amu.edu.pl*

Received: 08-08-2013

Abstract

3-(3-Dimethylammonio)propylammonio propanoate bromide (**1**), 4-(3-dimethylammonio)propylammonio butanoate bromide (**2**), and 5-(3-dimethylammonio)propylammonio pentanoate bromide (**3**) have been obtained in reaction of 1,1-dimethyl-1,3-propylenediamine with 3-bromopropionic acid, ethyl 4-bromobutyrate and 5-bromovaleric acid, respectively. The products have been characterized by FTIR, Raman and NMR spectroscopy. Also B3LYP calculations have been carried out. The screening constants for ^{13}C and ^{1}H atoms have been calculated by the GIAO/B3LYP/6-311G(d,p) approach and analyzed. Theoretical vibrational parameters are compared with obtained experimental parameters. Estimation of the pharmacotherapeutic potential has been accomplished for the synthesized compounds on the basis of Prediction of Activity Spectra for Substances (PASSs).

Keywords: Alkylammonium zwitterionic amino acids, FTIR, NMR spectra, PASS program, DFT calculations

1. Introduction

Amino acids are well known to exist as zwitterions in the crystalline state and in solutions. However, in the gas phase they are present in their neutral forms, which have been proved both experimentally and theoretically.[1,2] The zwitterionic form in the gas phase is stabilized by water; the more water molecules the more stable the complex.[3,4] In the solid state, the ammonium group of zwitterionic form usually interacts with carboxylate groups of other molecules, whereas in aqueous solutions hydrogen bondings occur between amino acids and surrounding water molecules.[5]

Amino acids and their complexes are of considerable chemical and biological interest. In proteins and peptides charge localization often stabilizes the formation of secondary and higher-order structure. They are also important for catalysis and ion transport.[6] Many functions of prokaryotic and eukaryotic cells depend on *N*-alkylated amino acids.[7–9] Potential pharmacological actions of compounds synthesized have been found on the basis of computer-aided drug discovery approaches with the Prediction of Activity Spectra for Substances (PASSs) program. It is based on a robust analysis of structure–activity relationships in a heterogeneous training set currently including about 60,000 biologically active compounds from different chemical series with about 4500 types of biological activity. Since only the structural formula of the chemical compound is necessary to obtain a PASS prediction, this approach can be used at the earliest stages of an investigation. There are many examples of the successful use of the PASS approach leading to new pharmacological agents.

The most important tools for structure investigations are vibrational spectroscopy methods.[10–16] However, the vibrational spectra of the zwitterionic amino acid derivatives are not yet fully understood, in spite of many papers devoted to the experimental and theoretical aspects of glycine[17] and glycine hydrochloride.[18]

One of the class of zwitterionic molecules are betaines, in which a carboxylate group is connected by one or more methylene groups with a quaternary nitrogen, $\geq N^{+}\text{-}(CH_2)_n\text{-}COO$. Betaines have a variety of applications in medicine, pharmacy and biology because of their biocidal properties.[19] Betaines which contain a hydrophobic chain in the range of n = 8–20 carbon atoms, show unique

properties as amphoteric surfactants. The main applications of alkyl betaines are in cosmetics and toiletries. Many of these compounds display very interesting physical properties, exhibiting phase transitions with ferroelectric, antiferroelectric and ferroelastic behaviour as well as phases with commensurate and incommensurate superstructures.[20]

In the case of zwitterionic species (amino acids and betaines) the cohesion forces in the crystals are dominated by COOH···X^- hydrogen bonds, N^+···X^- and N^+···O electrostatic interactions, and C-H···X^- contacts.[21] The electrostatic attractions depend on the number of methylene groups in the tether connecting the positively charged nitrogen atom with COO^- or COOH groups, counter anions, and also on additional substituents.[22] From the structural point of view, the new zwitterionic amino acids, containing additional aminopropyl group can be considered as bifunctional compounds.

In order to better understand the properties of bifunctional zwitterionic amino acids we synthesized a new series of 1,1-dimethylpropylene diamine derivatives.

The molecular structure of 3-(3-dimethylammonio)propylammonio propanoate bromide (**1**), 4-(3-dimethylammonio)propylammonio butanoate bromide (**2**) and 5-(3-dimethyl-ammonio)propylammonio pentanoate bromide (**3**) analyzed by FTIR and NMR spectroscopy and B3LYP calculations is presented in this paper. Additionally, the analyses of the biological prediction activity spectra for compounds **1**–**3** made herein are good examples of in silico studies of chemical compounds.

1–**3** belong to alkylammonium zwitterionic amino acid derivatives investigated in our laboratory in order to better understand the mechanism of their biological activity.

Another aspect of interest in alkylammmonium zwitterionic derivatives of 1,1-dimethyl-1,3-propylenediamine is the effect of the hydrocarbon chain length on the formation of zwitterionic amino acid derivatives in the solid state and as the isolated entities.

2. Experimental Procedure

2. 1. Instrumentation

The NMR spectra were measured with a Varian Gemini 300VT spectrometer, operating at 300.07 and 75.4614 MHz for ^{1}H and ^{13}C, respectively. Typical conditions for the proton spectra were: pulse width 32°, acquisition time 5 s, FT size 32 K and digital resolution 0.3 Hz per point, and for the carbon spectra pulse width 60°, FT size 60 K and digital resolution 0.6 Hz per point, the number of scans varied from 1,200 to 10,000 per spectrum. The ^{13}C and ^{1}H chemical shifts were measured in D_2O and are reported in δ (ppm) relative to an internal standard of 2,2,3,3-tetradeutero-3-trimethylsilylpropionic acid (TSP). Measurements in $CDCl_3$ are relative to an internal standard of TMS. All proton and carbon-13 resonances were assigned by ^{1}H (COSY) and ^{13}C (HETCOR). All 2D NMR spectra were recorded at 298 K on a Bruker Avance DRX 600 spectrometer operating at the frequencies 600.315 MHz (^{1}H) and 150.963 MHz (^{13}C), and equipped with a 5 mm triple-resonance inverse probe head [^{1}H/^{31}P/BB] with a self-shielded *z* gradient coil (90° ^{1}H pulse width 9.0 μs and ^{13}C pulse width 13.3 μs). FTIR spectra in Nujol and Fluorolube mulls and Raman spectrum were recorded on a Bruker IFS 66v/S spectrometer, evacuated to avoid water and CO_2 absorptions, at a 2 cm^{-1} resolution. Each FTIR spectrum consisted of 64 scans. The ESI (electron spray ionization) mass spectra were recorded on a Waters/Micromass (Manchester, UK) ZQ mass spectrometer equipped with a Harvard Apparatus syringe pump. The sample solutions were prepared in methanol at a concentration of approximately 10^{-5} M. The standard ESI-MS mass spectra were recorded at a 30 V cone voltage.

2. 2. Computational Details

The calculations were performed using the Gaussian 03 program package[23] and B3LYP[24,25] method in conjunction with 6-311G(d,p) basis set.[26] The biological activity spectra were predicted for all synthesized compounds using PASS.[27] The vibrational FTIR spectra (harmonic wavenumbers and absolute intensities) were calculated at the B3LYP/6-311G(d,p) level of theory. The magnetic isotropic shielding tensors were calculated using the standard GIAO/B3LYP/6-311G(d,p) (Gauge-Independent Atomic Orbital) approach.[28,29]

2. 3. Synthesis

3-(3-Dimethylammonio)propylammonio propanoate bromide (1)

1,1-Dimethylpropane-1,3-propylenediamine (5.12 g, 0.05 mol) was dissolved in ethanol (20 mL); 3-bromopropionic acid (7.65 g, 0.05 mol) dissolved in ethanol (20 mL) was added dropwise to the above solution while heated in boiling solvent for 27 h. The solvent was evaporated under reduced pressure and the residue was dried over P_4O_{10} and then recrystallized from anhydrous ethanol, yield 65%, m.p. 128–130 °C; Elemental analysis found (calcd.) C, 37.43 (37.66); H, 7.68 (7.51); N, 10.82 (10.98%); MS (EI, 20 eV): *m/z* (%) = 175 (M^+, 100); ^{1}H NMR (D_2O): δ = 2.19 (tt, 2H), 2.60 (t, 2H), 2.94 (s, 6H), 3.18 (t, 2H), 3.26 (t, 2H), 3.27 (t, 2H); ^{13}C NMR (D_2O): δ = 45.6 (CH_3), 47.3 (CH_2), 23.9 (CH_2), 46.7 (CH_2), 57.0 (CH_2), 35.2 (CH_2), 180.5 (C); FTIR: ν(C=O) at 1615 cm^{-1}. The deuterated sample was obtained by dissolving the compound in D_2O (twice), evaporating to dryness and recrystallized (twice) from CH_3OD.

4-(3-Dimethylammonio)propylammonio butanoate bromide (2)

1,1-Dimethylpropane-1,3-propylenediamine (5.12 g, 0.05 mol) was dissolved in ethanol (20 mL); ethyl 4-bromobut-

yrate (9.75 g, 0.05 mol) dissolved in ethanol (20 mL) was added dropwise to the above solution while heated in boiling solvent for 35 h. The solvent was evaporated under reduced pressure and the residue was dried over P_4O_{10} and then recrystallized from anhydrous ethanol, 49%, m.p. 153–155 °C; Elemental analysis found (calcd.) C, 39.93 (40.16); H, 7.72 (7.86); N, 10.30 (10.41%); MS (EI, 20 eV): *m/z* (%) = 189 (M^+, 100); ^{1}H NMR (D_2O): δ = 2.05 (tt, 2H), 2.08 (t, 2H), 2.90 (s, 6H), 3.17 (t, 2H), 3.53 (t, 2H), 3.38 (t, 2H); ^{13}C NMR (D_2O): δ = 45.5 (CH_3), 42.2 (CH_2), 24.8 (CH_2), 57.9 (CH_2), 50.8 (CH_2), 20.1 (CH_2), 33.6 (CH_2), 181.3 (C); FTIR: ν(C=O) at 1658 cm^{-1}.

5-(3-Dimethylammonio)propylammonio pentanoate bromide (3)

1,1-Dimethylpropane-1,3-propylenediamine (5.12 g, 0.05 mol) was dissolved in ethanol (20 mL); 5-bromovaleric acid (9.75 g, 0.05 M) dissolved in ethanol (20 mL) was added dropwise to the above solution while heated in boiling solvent for 50 h. The solvent was evaporated under reduced pressure and the residue was dried over P_4O_{10}. The compound was an oil; Elemental analysis found (calcd.) C, 41.76 (42.41); H, 8.11 (8.19); N, 9.75 (9.89%); MS (EI, 20 eV): *m/z* (%) = 203 (M^+, 100); ^{1}H NMR (D_2O): δ = 1.97 (tt, 2H), 1.63 (tt, 2H), 1.58 (tt, 2H), 2.30 (t, 2H), 2.87 (s, 6H), 3.13 (t, 2H), 3.29 (t, 2H), 3.61 (t, 2H) (Fig. 3 in Supporting Information); ^{13}C NMR (D_2O): δ = 45.6 (CH_3), 58.0 (CH_2), 24.6 (CH_2), 38.7 (CH_2), 63.9 (CH_2), 27.0 (CH_2), 38.1 (CH_2), 179.6 (C) (Fig. 4 in Supporting Information); FTIR: ν(C=O) at 1647 cm^{-1}.

3. Results and Discussion

3. 1. Synthesis

The reaction of 1,1-dimethylpropane-1,3-propylenediamine with 3-bromopropionic acid, ethyl 4-bromobutyrate and 5-bromovaleric acid leads to the protonation of dimethylamine group and substitution of the primary nitrogen atom by the hydrocarbon chain (Scheme 1). A similar reaction of 1,1-dimethylpropane-1,3-propylenediamine with ethyl chloroacetate in anhydrous ethanol gives 1,1-dimethyl-3-oxo-1,4-diazepan-1-ium chloride whereas quaternization with chloroacetic acid yields 1,1-dimethyl-1-carboxymethyl-3-aminopropylammonium hydrochloride.[30] The different reaction routes of 1,1-dimethylpropane-1,3-propylenediamine with chlorocarboxylic acid and bromocarboxylic acid derivatives are caused by the difference of the acid strength.

3. 2. B3LYP Calculations

The structure and numbering of carbons for **1**–**3** are given in Scheme 1. The energy, dipole moments and selected geometry parameters were calculated at the B3LYP /6-311G(d,p) level of theory and are presented in Table 1.

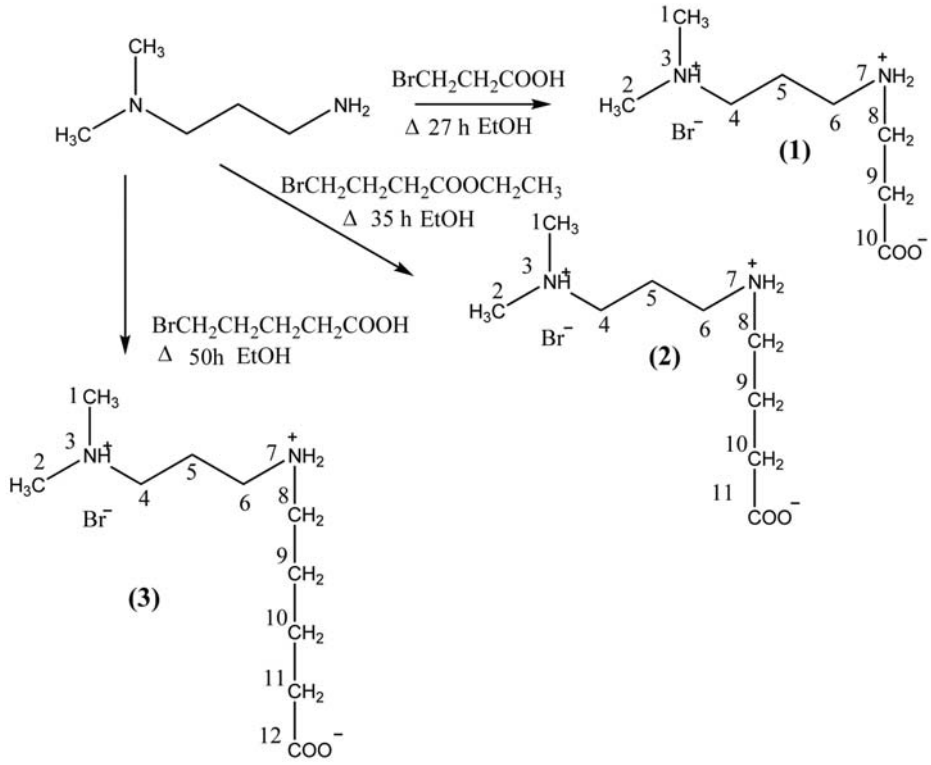

Scheme 1. Synthesis of 3-(3-dimethylammonio)propylammonio propanoate bromide (**1**), 4-(3-dimethylammonio)propylammonio butanoate bromide (**2**), 5-(3-dimethylammonio)propylammonio pentanoate bromide (**3**).

Table 1. Calculated structural parameters (B3LYP/6-311G(d,p)) for 3-(3-dimethylammonio)propylammonio propanoate bromide (**1**), 4-(3-dimethyl-ammonio)propylammonio butanoate bromide (**2**), 4-(3-dimethyl-ammonio)propylammonio butanoate bromide monohydrate (**2a**), 5-(3-dimethylammonio)propylammonio pentanoate bromide (**3**) and 5-(3-dimethylammonio)propylammonio pentanoate bromide monohydrate (**3a**) estimated by B3LYP/6-311G(d,p) calculations.

Parameters	**1**	**2**	**2a**	**3**	**3a**
Energy(a.u.)	–3147.96743543	–3189.90763248	–3263.77768535	–3226.63117702	–3303.06504282
Dipol moment (Debye)	12.5100	7.2234	6.9794	11.5273	12.7675
Bond lengths [Å]					
N(3)–H	1.022	1.136	1.051	1.147	1.033
N(7)–H(1)	1.134	1.734	1.575	1.793	1.551
N(7)–H(2)	1.070	1.018	1.036	1.020	1.020
C(10)–O(1)	1.220	1.203	1.219	1.211	1.208
C(10)–O(2)	1.318	1.342	1.335	1.344	1.351
C(1)–N(3)	1.505	1.483	1.493	1.483	1.503
C(2)–N(3)	1.508	1.484	1.501	1.483	1.505
N(3)–C(4)	1.544	1.495	1.515	1.497	1.521
Angles [deg]					
C(1)–N(3)–C(4)	117.1	114.3	109.7	112.0	114.0
C(9)–C(10)–O(2)	113.6	117.1	116.6	115.8	115.3
C(4)–C(5)–C(6)	117.3	111.0	118.0	111.0	120.0
C(6)–N(7)–C(8)	117.0	114.9	116.1	115.7	113.5
N(7)–C(8)–C(9)	108.6	112.0	120.0	111.7	112.9
Dihedral angles [deg]					
N((7)–C(8)–C(9)–C(10)	–52.0	–70.5	067.4	–89.4	–73.2
C(8)–C(9)–C(10)–O(2)	40.3	–	–	–	–
N(3)–C(4)–C(5)–C(6)	81.5	–177.8	88.4	–167.7	57.3
C(4)–C(5)–C(6)–N(7)	37.9	178.4	–64.5	174.8	55.6
C(1)–N(3)–C(4)–C(5)	–32.9	–64.4	175.8	167.5	47.2
C(8)–C(9)–C(10)–C(11)	–	85.0	74.7	–	–
Hydrogen bonds and short contacts lengths					
Distances [Å]					
N(7)–H(2)··· Br (Å)	3.126	–	3.299	–	–
N(7)–H(1)··· O (Å)	2.484	2.720	2.575	2.774	2.512
N(3)–H··· O (Å)	3.227	–	3.475	3.005	2.812
N(3)···H···Br	–	3.022	3.173	–	–
N(3) ···O(2)	3.142	–	–	–	–
Angles [deg]					
N(7)–H··· Br (Å)	159.5	–	176.4	–	–
N(7)–H··· O (Å)	160.2	170.0	–	167.5	166.5
N(3)–H··· O (Å)	–	–	111.6	–	152.8
N(3) ···H···Br	–	177.4	–	178.3	–

The structures optimized at the B3LYP/6-311G(d,p) level of theory for **1–3** are shown in Fig. 1.

In **1** the NH_2^+R group forms a weak hydrogen bond with the bromide anion; N(7)–H(2)···Br = 3.l126 Å and protons of this group are not equivalent (Table 1). The positively charged nitrogen atoms are engaged in an intramolecular interaction with the COO^- group N(7)–H(1)···O = 2.484 Å, N(3)–H(1)···O = 3.227 Å. Additionally, the nitrogen atom $N^+(3)$ interacts *via* Coulombic attractions with the adjacent negatively charged oxygen atom (Table 1). The compound **2** does not have the structure of a zwitterion in the gas phase. Nitrogen atom is engaged in a hydrogen bond N(7)···H(2)···O, 2.720 Å while the bromide anion forms a linear hydrogen bond N(3)–H···Br = 3.022 Å. Similarly, compound **3** does not have a form of a zwitterion. Moreover, the structure of **1** has the highest energy among the investigated compounds **1–3**. The calculated energy for **1** is about 1.3% higher than for **2** and 2.5% higher in comparison to compound **3** (Table 1). The high tendency to form neutral molecules arises from the much lower energy of compounds **2** and **3** in comparison to the compound **1**. Compounds in which the carboxylate group is protonated are much more stable in terms of thermodynamics. The calculated bond lengths and bond angles for **1–3** are similar, however the torsion angles are substantially different. This shows a crucial role of the proton position in the structure of the investigated compounds (Table 1). These data prove that in the

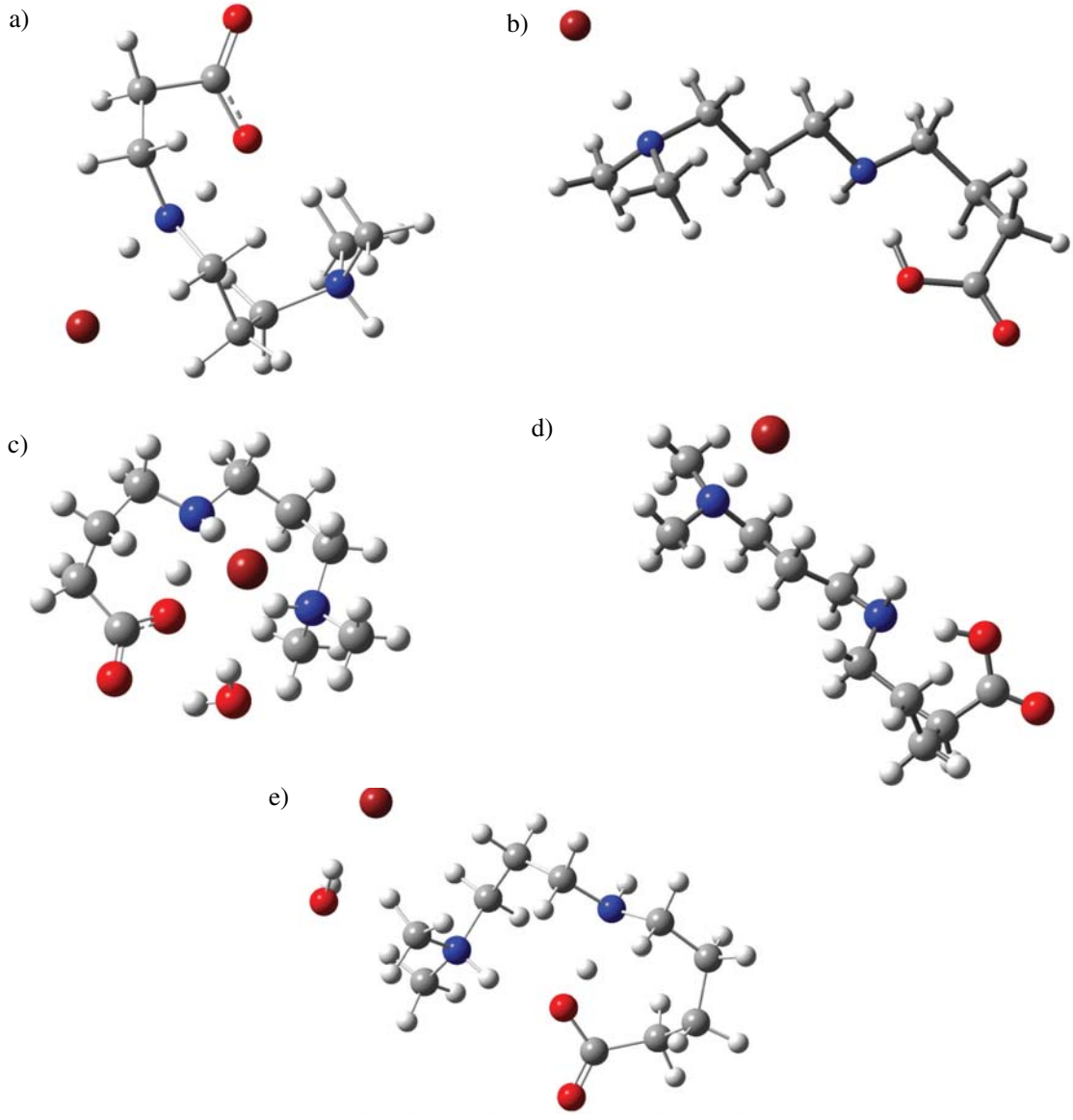

Figure 1. Structures of a) 3-(3-dimethylammonio)propylammonio propanoate bromide (**1**), b) 4-(3-dimethylammonio)propylammonio butanoate bromide (**2**), c) 4-(3-dimethylammonio)propylammonio butanoate bromide monohydrate (**2a**), d) 5-(3-dimethylammonio)propylammonio pentanoate bromide (**3**) and e) 5-(3-dimethylammonio)propylammonio pentanoate bromide monohydrate (**3a**) calculated by the B3LYP/6-311G(d,p) method.

gas phase the zwitterionic form plays an important role in the molecular structure of the compound **1** in contrast to the compounds **2** and **3**, where the stabilization is achieved by the neutral form of the compound. The calculated structures of 4-(3-dimethyl-ammonio)propylammonio butanoate bromide monohydrate (**2a**) and 5-(3-dimethylammonio)propylammonio pentanoate bromide monohydrate (**3a**) are significantly different than their non-hydrated analogues which confirms that molecules of water stabilize the structure of zwitterions in the gas phase (Figs 1c and 1e).[31] In the most cases energy of hydrated clusters is lower in comparison to non-hydrated compounds (Table 1).

3. 3. The Predicted Biological Activity

The biological activity spectra were predicted for all three synthesized compounds **1**–**3** using PASS. They were also selected the types of activities that were predicted for a potential compound with the highest probability (focal activities) (Table 1 in Supporting Information). According to these data the most frequently predicted types of biological activity are creatinase inhibition, polyamine-transporting ATPase inhibitor, hydrogen dehydrogenase inhibitor, and alkylacetylglycero-phosphatase inhibition, mucositis treatment, antiviral, antitoxic and antimutagenic agents.

3. 4. ^{1}H NMR and ^{13}C NMR Spectra

The proton chemical shift assignments (Table 2) are based on 2D COSY experiments, in which the proton-proton connectivity is observed through the off-diagonal peaks in the counter plot (Fig. 2 in Supporting Information).

The carbon chemical shifts assignments were based on the heteronuclear correlation ^{1}H-^{13}C (HETCOR) experiments (Fig. 2 and Fig. 1 in Supporting Information).[32] The relation between the experimental ^{13}C and ^{1}H chemical shifts (δ_{exp}) and the Gauge-Independent Atomic Orbitals (GIAO) magnetic isotropic shielding constants (σ_{calc}) are usually linear and are described by the equation: $\delta_{exp} = a + b\,\sigma_{calc}$.[33–35] This relationship is shown in Fig. 3.

The slope and intercept of the least-square correlation lines are used to scale the GIAO isotropic absolute shielding constants σ, and to predict chemical shifts in D_2O (Fig. 3, Table 2).

The relations between the experimental ^{1}H and ^{13}C chemical shifts (δ_{exp}) and the GIAO (Gauge-Independent Atomic Orbitals) isotropic magnetic shielding tensors

Table 2. Chemical shifts (δ, ppm) in D_2O calculated by GIAO nuclear magnetic shielding constants (σ_{calc}) for 3-(3-dimethylammonio)propylammonio propanoate bromide (**1**), 4-(3-dimethylammonio)propylammonio butanoate bromide (**2**) and 5-(3-dimethylammonio)propylammonio pentanoate bromide (**3**). The predicted GIAO chemical shifts were computed from the linear equation $\delta_{exp.} = a + b\cdot\sigma_{calc}$ with a and b determined from the fit of the experimental data (r is the correlation coefficient).

	$\delta_{exp.}$	δ_{calc}	σ_{calc}		$\delta_{exp.}$	δ_{calc}	σ_{calc}
3-(3-dimethylammonio)propylammonio propanoate bromide (**1**)							
carbon-13			*proton*				
C(1,2)	45.6	149.39	44.0	H(1,2)	2.94	2.76	29.14
C(4)	47.3	131.67	63.9	H(4)	3.18	3.02	28.54
C(5)	23.9	166.37	25.0	H(5)	2.19	2.50	29.73
C(6)	46.7	146.59	47.2	H(6)	3.27	3.08	28.40
C(8)	57.0	146.94	46.8	H(8)	3.30	3.53	27.37
C(9)	35.2	160.78	31.2	H(9)	2.60	2.58	29.56
C(10)	180.5	30.17	178.0				
a[a]		211,8951				15.4419	
b[b]		–1.1236				–0.4352	
r^{2}[c]		0.9760				0.7478	
4-(3-dimethylammonio)propylammonio butanoate bromide (**2**)							
carbon-13			*proton*				
C(1,2)	45.5	144.04	35.8	H(1,2)	2.90	29.68	2.82
C(4)	50.8	127.74	53.8	H(4)	3.17	29.33	3.24
C(5)	24.8	158.55	19.7	H(5)	2.08	30.33	2.04
C(6)	42.2	131.72	49.4	H(6)	3.38	29.40	3.15
C(8)	57.9	127.12	54.4	H(8)	3.53	29.17	3.43
C(9)	20.1	154.52	24.2	H(9)	2.05	30.36	2.00
C(10)	33.6	141.43	38.6	H(10)	2.47	29.61	2.90
C(11)	181.3	13.08	180.4				
a[a]		194.8155				38.4396	
b[b]		–1.1043				–1.2002	
r^{2}[c]		0.9875				0.8807	
5-(3-dimethylammonio)propylammonio pentanoate bromide (**3**)							
carbon-13			*proton*				
C(1,2)	45.6	151.87	43.41	H(1,2)	2.87	29.49	2.65
C(4)	58.0	136.43	60.67	H(4)	3.13	29.42	2.77
C(5)	24.6	167.12	26.37	H(5)	1.97	29.38	2.84
C(6)	38.7	143.57	52.69	H(6)	3.29	29.13	3.29
C(8)	63.9	143.22	53.08	H(8)	3.61	29.09	3.36
C(9)	38.1	164.43	29.49	H(9)	1.63	30.05	1.65
C(10)	27.0	162.27	31.79	H(10)	1.58	30.12	1.52
C(11)	38.1	156.84	37.86	H(11)	2.30	29.69	2.29
C(12)	179.6	30.73	178.79				
a[a]		213.1289				55.3057	
b[b]		–1.1175				–1.17856	
r^{2}[c]		0.9766				0.7657	

[a] intercept; [b] slope; [c] correlation coefficient

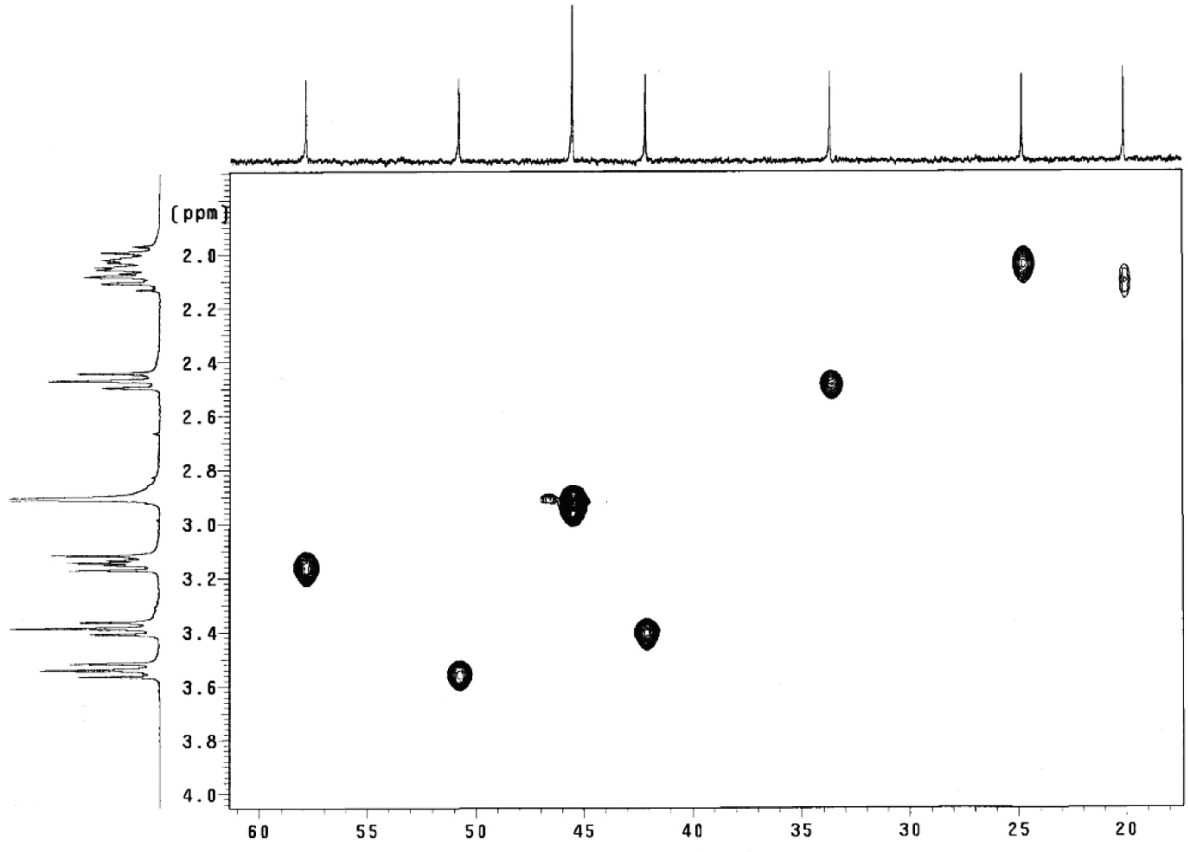

Figure 2. $^{1}H–^{13}C$ (HETCOR) of 4-(3-dimethylammonio)propylammonio butanoate bromide (**2**).

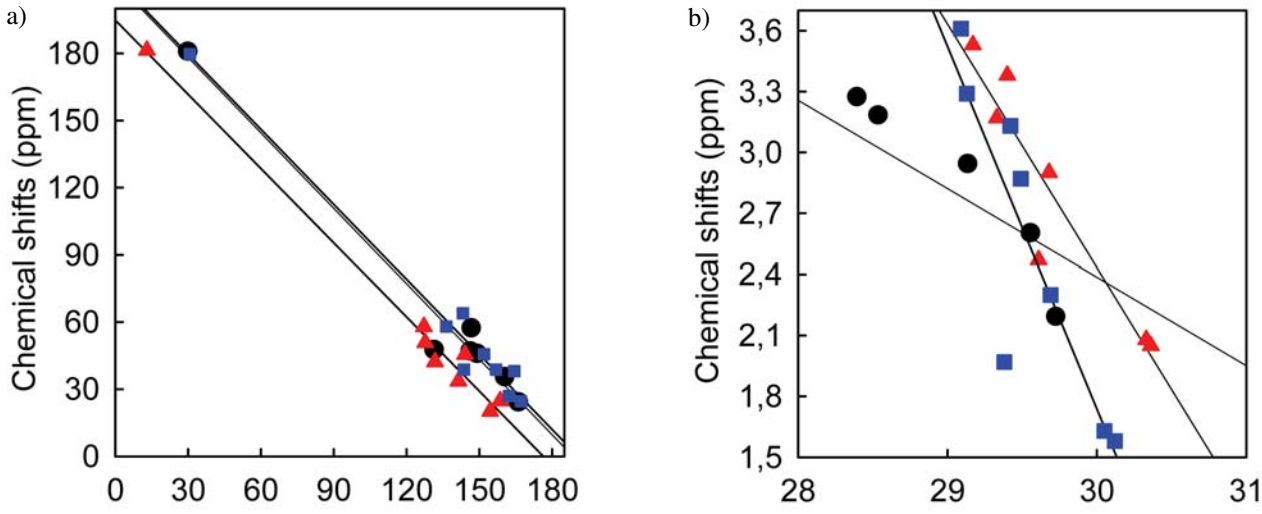

Figure 3. Experimental chemical shifts (δ_{exp}, D_2O) in for 3-(3-dimethylammonio)propylammonio propanoate bromide (**1**) (●), 4-(3-dimethylammonio)propylammonio butanoate bromide (**2**) (▲) and 5-(3-dimethylammonio)propylammonio pentanoate bromide (**3**) (■) *vs.* isotropic magnetic shielding constants (σ_{calc}) from the GIAO/B3LYP/6-311G(d,p) calculations; (a) carbons-13 and (b) protons.

(σ_{calc}) for **1**–**3** are linear and the a and b parameters are given in Table 2. As can be seen from Fig. 3 the agreement between the experimental and the calculated data for protons is worse than for carbons-13.[36] The protons are located on the periphery of the molecule, thus their interactions with solvent molecules are much stronger than interactions of more hidden carbon atoms. The differences between the calculated and experimental shifts for protons are probably due to the fact that the shifts are calculated for single molecules in the gas phase.

3. 5. FTIR and Raman Spectra

Room-temperature solid-state FTIR and Raman spectra as well as the calculated spectra of **1** are shown in Fig. 4. The band frequencies, relative intensities and their assignments in the range 4000–400 cm^{-1} are listed in Table 3. For convenience of comparison, the band intensities for the calculated spectrum are scaled. The strong absorption of **1** in the 3070–2370 cm^{-1} region corresponds to the $\nu(N^+H\cdots^-O)$ band which is a typical absorbance for hydrogen bonds with an N···O distance between 2.4 and 2.5 Å (Fig. 4a).

The absorption shifts to lower frequencies after deuteration and one broad band at 2250–1890 cm^{-1} which corresponds to the ND group is observed. No absorption of NH group is observed in the Raman spectrum (Fig. 4b).

When the proton of NH group is replaced by deuterium, bands at 1445 and 992 cm^{-1} are shifted to 1100 and 687 cm^{-1}, respectively (Fig. 4a). It appears that these bands correspond to the NH and ND in-plane and out-of-plane bending modes. The $\nu_{as}(COO^-)$ and $\nu_s(COO^-)$ for 3-(3-dimethylammonio)propylammonio propanoate bromide (**1**) are located at 1615 and 1385 cm^{-1} and they have the slightly higher wavenumbers in comparison to betaines[37]

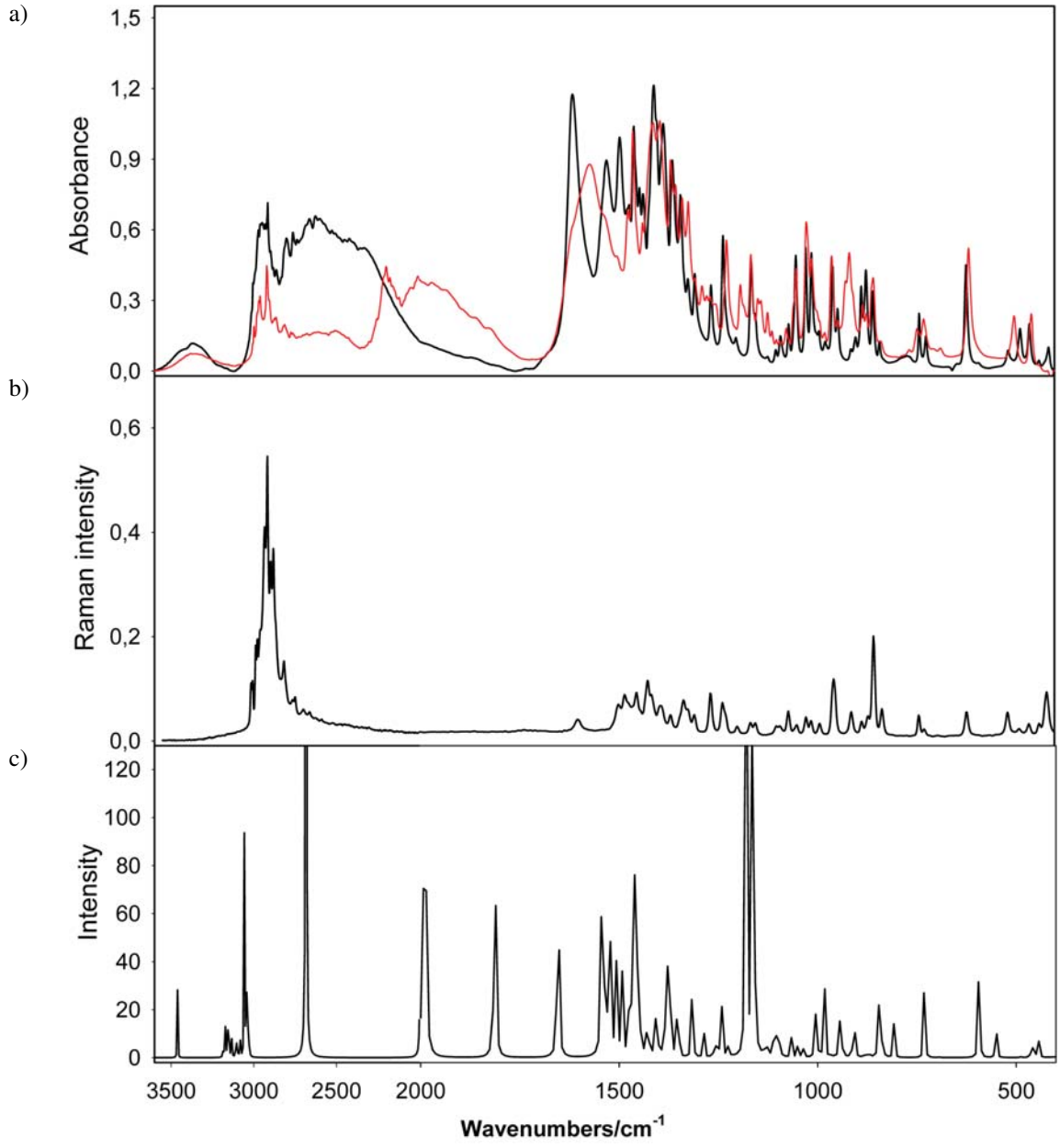

Figure 4. Spectra of 3-(3-dimethylammonio)propylammonio propanoate bromide (**1**): (a) FTIR (suspension in Nujol and Fluorolube, red line – deuterated analogue), (b) Raman spectrum and (c) calculated scaled FTIR spectrum.

Table 3. Observed and calculated B3LYP/6-311G(d,p) vibrational frequencies and infrared intensities for 3-(3-dimethylammonio)propylammonio propanoate bromide (**1**).

Raman	IR(exp.)	IR(exp. deut)	IR(calc.)	INT	IR(scaled)	Proposed assignment
	3413vw	3425vw	3467	28.7	3301	ν(NH)
3047vw	3036w	3030vw	3189	15.0	3033	$\nu(CH_3)$
3038vw						
3008w	3002m	2999w	3178	12.5	3022	$\nu(CH_3)$
2963m	2991m	2991m	3164	33.3	3008	$\nu(CH_3)$
2946s	2979m	2950w	3138	11.9	2983	$\nu(CH_2)$
2925m	2960m	2934w	3105	7.25	2951	$\nu(CH_2)$
2909m	2890–2300	2250–1890	3065	50.2	2913	$\nu(N^+–H \cdot O)$
2842w	broad	broad	3053	14,6	2901	
2788vw			2689	1483	2550	
			1993	520	1878	
1600	1615s	1569s	1817	243	1708	$\nu_{as}(COO)$
	1529m	1530m	1657	208	1554	ν(NH)
1497	1495m	1502m	1551	7.41	1451	$\nu(CH_2)$
1482w	1471w	1474m	1524	40.4	1425	$\nu(CH_2)$
1452w	1460m	1460s	1511	44.5	1413	$\beta_{as}CH_3$, $\delta(CH_2)$
	1445w	1100w	1499	13.0	1401	δ(OH), δ(NH)
1424vw	1435w	1436w	1494	34.8	1396	$\delta(CH_2)$
1414vw	1408s	1410s	1479	21.1	1382	νOH
1391vw	1401s	1393s	1468	92	1371	$\beta_s CH_3$
	1385s	1366m	1461	284	1364	νOH
1366vw	1361s	1354m	1453	60	1357	ν(CC)
1333vw	1341w	1336m	1434	10.6	1338	δ(HOH)
1323w	1323vw	1321vw	1424	11.5	1329	ν(CC)
1306vw	1305vw	1305vw	1409	45.8	1314	ν(CC)
1265w	1264vw	1286vw	1383	141	1289	ν(CC)
		1276vw				
		1253vw				
1235vw	1234w	1225w	1356	24.8	1263	$\omega(CH_2)$
1199vw	1202vw	1190vw	1350	4.1	1257	$\tau(CH_2)$
1165vw	1163w	1164w	1318	35.5	122	ν(CC)
1153vw	1154vw	1146vw	1289	9.8	1198	ν(CC)
	1122vw	1139vw	1261	15.2	1171	ν(CC)
1100vw	1102vw	1122vw	1245	48.0	1156	ν(CC)
1191vw	1090vw	1110vw	1227	6.45	1138	ν(CC)
1169vw	1069vw	1090vw	1183	228	1096	ν(CC), $\beta(CH_2)$
		1075vw				
1048vw	1051w	1050w	1176	1.94	1089	ν(CO)
1025vw	1026m	1025w	1165	421	1079	ν(CN)
1013vw	1012m	1011w	1132	18.3	1047	ν(CC)
991vw	992vw	687vw	1097	10.9	1013	β(OH)
	977vw	978vw	1068	8.13	985	ν(CC)
995w	958m	961w	1053	4.58	970	ν(CN)
	945w	945vw	1039	8.17	957	ν(CC)
911vw	912vw	926vw	1006	40.5	925	ν(CC), $\beta(CH_2)$
	901vw	916w	985	37.2	905	$\beta(CH_2)$
885vw	886w	882vw	966	2.27	886	$\beta(CH_2)$
869vw	874m	873vw	944	49.9	865	ν(CC)
855m	857w	855w	911	36.5	833	ν(CC), ν(CN)
834vw	840vw	837vw	882	3.38	805	ν(CC)
	770vw	765vw	873	4.56	797	ν(CN)
741vw	740vw	746vw	845	85	770	ν(CN)
727vw	723vw	729vw	809	14.1	735	ν(CN)
	644vw		733	28.8	662	$\gamma(CH_2)$
621vw	623m	616w	697	0.41	627	$\gamma(CH_2)$
	591vw		595	52	528	$\gamma(CH_2)$

Raman	IR(exp.)	IR(exp. deut)	IR(calc.)	INT	IR(scaled)	Proposed assignment
517vw	516vw	501vw	551	14.8	486	$\beta(CH_2)$, τ(CN)
488vw	486vw		489	0.36	426	β(CCC)
464vw	463vw	458vw	461	12.5	399	β(CO)
438vw	439vw		446	16.8	384	$\gamma(CH_2)$
419w	415vw		386	2.65	327	$\gamma(CH_2)$
344vw			350	180	292	β(CCC)
275vw			293	0.98	237	β(CCC)
245vw			286	2.59	230	τring
200vw			233	8.22	179	Lattice mode
165vw			173	9.95	121	Lattice mode
147w			160	12.0	108	Lattice mode
92vw			110	3.46	60	Lattice mode
68w			85	14.9	36	Lattice mode

The abbreviations are: s: strong, m: medium, w: weak, vw: very weak, ν: stretching, β: in plane bending, δ: deformation, ω: wagging, γ: out of plane bending and τ: twisting.

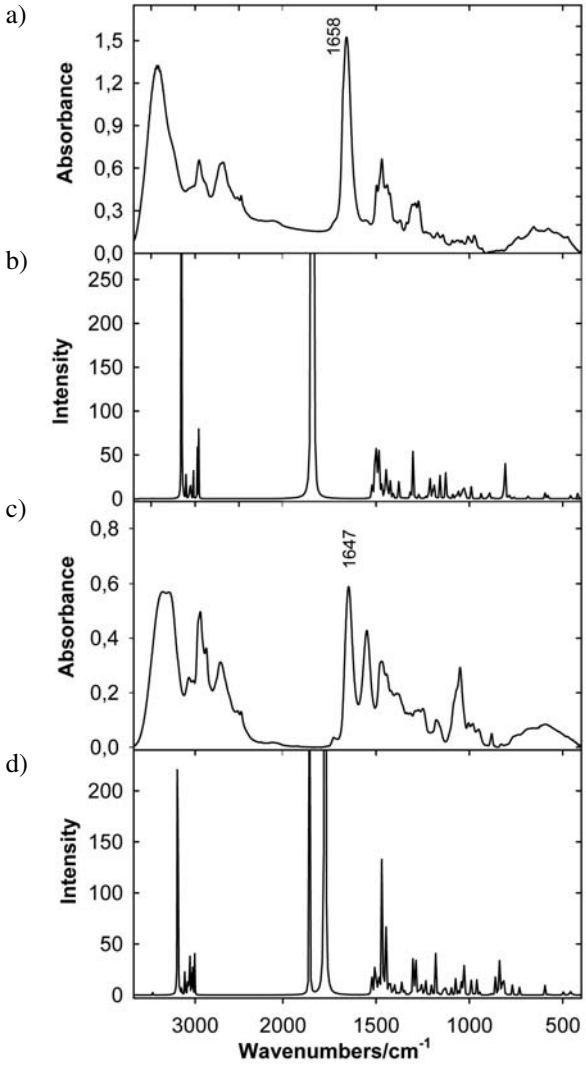

Figure 5. Spectra of 4-(3-dimethylammonio)propylammonio butanoate bromide (**2**): (a) FTIR (suspension in Nujol and Fluorolube), (b) calculated unscaled spectrum and spectra of 5-(3-dimethylammonio)propylammonio pentanoate bromide (**3**): (c) FTIR (suspension in Nujol and Fluorolube), (d) calculated unscaled spectrum.

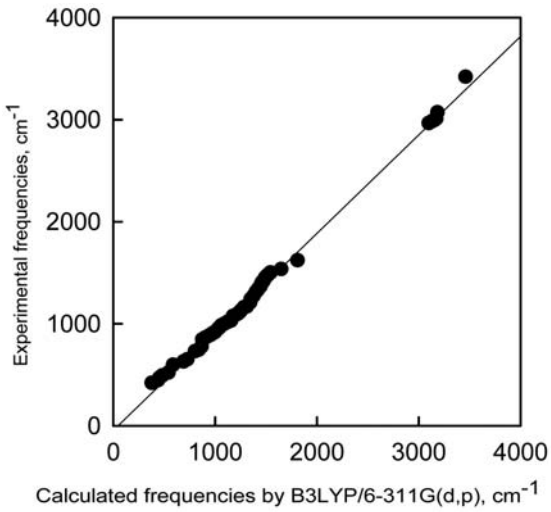

Figure 6. Correlation between the experimental and calculated wavenumbers (cm^{-1}) for 3-(3-dimethylammonio)propylammonio propanoate bromide (**1**); $\nu_{scaled} = -45.5971 + 0.9654\ \nu_{calc.}$, $r^2 = 0.9967$.

and amino acids.[38,39] This absorption shifts to higher wavenumbers, 1658 cm^{-1} and 1647 cm^{-1} for **2** and **3**, respectively (Fig. 5a, 5c). The DFT harmonic vibrational wavenumbers for COO groups for **2** and **3** are higher than the experimental vibrational frequency because in the gas phase carboxylate group is protonated (Fig. 5b and 5c). The DFT harmonic vibrational wavenumbers are usually higher than the experimental values. However, in this case the overall agreement between the experimental and calculated frequencies for **1** is very good (Fig. 6).

Any discrepancy noted between the observed and calculated frequency may be due to the fact that the calculations have been done for a single molecule in the gaseous state contrary to the experimental spectrum recorded in the presence of intermolecular interactions. The scaling procedure, as recommended by Alcolea Palafox was used.[40,41] The scaled IR spectrum is shown in Fig. 4c and

the predicted frequencies are listed in Table 3 as ν_{scaleq}. Scaling of the harmonic vibrational frequencies reproduced the experimental solid-state FTIR frequencies with the r.m.s. error of 38.1 cm^{-1}. The vibrational band assignments of **1–3** was made using Gauss-View molecular visualization program.[42]

4. Conclusions

Quaternization of 1,1-dimethyl-1,3-propylenediamine with 3-bromopropionic acid, gives 3-(3-dimethylammonio)propylammonio propanoate bromide (**1**), with ethyl 4-bromobutyrate gives 4-(3-dimethylammonio)propylammonio butanoate bromide (**2**) and with 5-bromovaleric acid gives 5-(3-dimethylammonio)propylammonio pentanoate bromide (**3**). The effects of inter- and intramolecular interactions and conformation of molecules have been precisely explained by comparison of experimental data taken in the condensed phase and calculated data (gas phase). The influence of acid strength on the structure of alkylammonium zwitterionic amino acid derivatives has also been shown. Using the PASS computer program the biological activity spectra of the synthetized compounds have been estimated. The structure of the investigated compounds **1–3** has been determined by FTIR, Raman, NMR spectroscopy and B3LYP calculations. In the gas phase the position of the proton has a crucial role in the structure of the investigated compounds. For compounds **2** and **3** the zwitterionic structure in the gas phase can be totally different from that in the condensed phase. The FTIR spectra of the investigated compounds **1–3** correspond very well to the structures optimized by B3LYP calculations. Linear correlations between the experimental ^{1}H and ^{13}C chemical shifts and the computed screening constants confirm the optimized geometry.

5. Acknowledgements

This work was supported by the funds from Adam Mickiewicz University, Faculty of Chemistry.

6. References

1. A. G. Császar, *J. Mol. Struct*. **1995**, *346*, 141–152.
2. M. T. Rosado, M. Leonor, T. S. Duarte, R. Fausto, *Vibrat. Spectrosc*. **1998**, *16*, 35–54.
3. J. H. Jensen, M. S. Gordon, *J. Am. Chem. Soc* **1995**, *117*, 8159–8170.
4. Y. Ding, K. J. Knogh-Jespersen, *Comput. Chem*. **1996**, *17*, 338–349.
5. P. Cyrac, A. Anand, G. Kumaresan, S. Vimalan, M. Gunasekaran, S. Madhavan, J. Growth, *Arch. Appl. Sci. Research* **2010**, *2(2),* 223–232.
6. A. White, P. Handler, E. L. Smith, *Principles of Biochemistry*. Mc-Graw-Hill, New York, **1968**.
7. A. Barth, *Prog. Biophys Mol. Biol.***2000**, *74*, 141–173.
8. J. Hlavacek, I. Fric, M. Budesinsky, K. Blaha, *Collect. Czech. Chem. Commun.* **1988**, *53*, 2473–2494.
9. B. Z. Chowdhry, T. J. Dines, S. Jabeen, R. Withnall, *J. Phys. Chem.* **2008**, *112*, 10333–10347.
10. A. Trivella, T. Gaillard, R. H. Store, P. Hellwing, *J. Chem. Phys.* **2010**, *132*, 115105–115116.
11. N. Kausar, T. J. Dines, B. Z. Chowdhry, B. D. Alexander, *Phys. Chem. Chem. Phys*. **2009**, *11*, 6389–6400.
12. M. W. Forbes, M. F. Bush, N. C. Polfer, J. Oomens, R. C. Dunbar, E. R. Williams, R. A. Jockusch, *J. Phys. Chem. A* **2007**, *111*, 11759–11770.
13. K. M. Harmon, G. F. Avci, *J. Mol. Struct*. **1984**, *117*, 295–302.
14. N. X. Cao, G. Fischer, *J. Phys. Chem*. **1999,** *103*, 9995–10003.
15. J. Sun, H. Forbert, D. Bosquet, D. Marx, *J. Chem. Phys*. **2010**, *133*, 114508–114521.
16. Z. Cao, G. Fisher, *J. Mol. Struct*. **2000**, *519*, 153–163.
17. J. Baran, A. J. Barnes, H. Ratajczak, *J. Mol. Struct*. **2012**, *1009*, 55–68.
18. S.-G. Ang, M. P. Williamson, D. H. Williams, J. *Chem. Soc. Perkin Trans 1*, **1988**, 1949–1956.
19. X. Domingo, *Amphoteric Surfactants*, ed. E. G. Lomax, Marcel Dekker, New York **1996**, pp. 76–190.
20. G. Schaack, *Ferroelectrics* **1990**, *104*, 147–158.
21. M. Szafran, I. Kowalczyk, J. Koput, A. Katrusiak, *J. Mol. Struct*. **2005**, *744–747*, 59–67.
22. M. Szafran, I. Kowalczyk, A. Katrusiak, *J. Mol. Struct*. **2006**, *786*, 25–32.
23. R. Dennington II, T. Keith, T. J. Millam, *Gauss View, Version 4.1.2,* Semichem. Inc., Shawnee Mission, KS, **2007**.
24. M. J. Frisch, G. W. Trucks, H. B. Schlegel, G. E. Scuseria, M. A. Robb, J. R. Cheeseman, J. A. Montgomery, Jr., T. Vreven, K. N. Kudin, J. C. Burant, J. M. Millam, S. S. Iyengar, J. Tomasi, V. Barone, B. Mennucci, M. Cossi, G. Scalmani, N. Rega, G. A. Petersson, H. Nakatsuji, M. Hada, M. Ehara, K. Toyota, R. Fukuda, J. Hasegawa, M. Ishida, T. Nakajima, Y. Honda, O. Kitao, H. Nakai, M. Klene, X. Li, J. E. Knox, H. P. Hratchian, J. B. Cross, C. Adamo, J. Jaramillo, R. Gomperts, R. E. Stratmann, O. Yazyev, A. J. Austin, R. Cammi, C. Pomelli, J. W. Ochterski, P. Y. Ayala, K. Morokuma, G. A. Voth, P. Salvador, J. J. Dannenberg, V. G. Zakrzewski, S. Dapprich, A. D. Daniels, M. C. Strain, O. Farkas, D. K. Malick, A. D. Rabuck, K. Raghavachari, J. B. Foresman, J. V. Ortiz, Q. Cui, A. G. Baboul, S. Clifford, J. Cioslowski, B. B. Stefanov, G. Liu, A. Liashenko, P. Piskorz, I. Komaromi, R. L. Martin, D. J. Fox, T. Keith, M. A. Al-Laham, C. Y. Peng, A. Nanayakkara, M. Challacombe, P. M. W. Gill, B. Johnson, W. Chen, M. W. Wong, C. Gonzalez, J. A. Pople, *GAUSSIAN 03*, Revision B.05, Gaussian, Inc., Pittsburgh PA, **2004**.
25. A. D. Becke, *J. Chem. Phys*., **1997**, *107*, 8554–8560 and references cited therein.

26. P. J. Stephens, F. J. Devlin, C. F. Chabalowski, M. J. Frisch, *J. Phys. Chem*. **1994**, *98*, 11623–11627.
27. (a) Pharma Expert Predictive Services Version 2.0 © 2011–2013. Available online: http://www.pharmaexpert.ru/PASSOnline/ (accessed on 1 November 2013); (b) V. V. Poroikov, D. A. Filimonov; Y. V. Borodina, A. A. Lagunin, A. J. Kos, *Chem. Inf. Comput. Sci*., **2000**, *40*, 1349–1361; (c) V. V. Poroikov, D. A. Filimonov, *J. Comput. Aided Mol. Des*. **2003**, *16*, 819–832; (d) V. V. Poroikov, D. A. Filimonov, in: *Predictive Toxicology*; C. Helma, Ed.; Taylor and Francis, **2005**, pp 459–478; (e) A. V. Stepanchikova, A. A. Lagunin, D. A. Filimonov, V. V. Poroikov, *Curr. Med. Chem*., **2003**, *10*, 225–238.
28. W. J. Hehre, L. Random, P. v. R. Schleyer, J. A. Pople, *Ab Initio Molecular Orbital Theory*, Wiley, New York, **1989**.
29. K. Wolinski, J. F. Hilton, P. J. Pulay, *J. Am. Chem. Soc*. **1990**, *112*, 8251–8260.
30. I. Kowalczyk, *Molecules* **2008**, *13*, 379–390.
31. I. Kowalczyk, *J. Mol. Struct*. **2010**, *973 (1–3)*, 163–171.
32. H. Simpson, *Organic Structure Determination Using 2-D NMR Spectroscopy*, Academic Press Elsevier, Amsterdam, **2008**.
33. R. Ditchfield, *Mol. Phys*. **1974**, *27*, 789–807.
34. A. Forsyth, A. B. Sabag, *J. Am. Chem. Soc*. **1997**, *119*, 9483–9494.
35. B. Ośmiałowski, E. R. Kolehmainen, R. Gawinecki, *Magn. Res. Chem.* **2001**, *39*, 334–340 and references cited therein.
36. A. R. Katritzky, N. G. Akhmedov, A. Gűven, E. F. V. Scriven, S. Majumder, R. G. Akhmedova, C. D. Hall, *J. Mol. Struct.* **2006**, *783*, 191–203.
37. Z. Dega-Szafran, Z. Kosturkiewicz, E. Nowak, M. Petryna, M. Szafran, *J. Mol. Struct.* **2002**, *613*, 37–45.
38. M. Rozenberg, G. Shoham, *Biophys. Chem.* **2007**, *125*, 166–203.
39. R. Wu, T. B. McMahon, *Angew. Chem. Int. Ed.* **2007**, *46*, 3668–3671.
40. M. Alcolea Palafox, *Int. J. Quant. Chem.* **2000**, *77(3)*, 661–684.
41. M. Alcolea Palafox, N. Iza, *Phys. Chem. Chem. Phys*., **2010**, *12*, 881–893.
42. P. Pulay, X. Zhou, F. Fogarasi, in: *Recent Experimental and Computational Advances in Molecular Spectroscopy*, R. Fausto, Ed.; Kluver Academic, Netherlands, **1993**, pp. 88–111.

Povzetek

3-(3-Dimetilamonio)propilamonio propanoat bromid (**1**), 4-(3-dimetilamonio)propilamonio butanoat bromid (**2**) in 5-(3-dimetilamonio)propilamonio pentanoat bromid (**3**) smo pripravili z reakcijo med 1,1-dimetil-1,3-propilendiaminom in 3-bromopropanojsko kislino, etil 4-bromobutiratom oz. 5-bromovalerijansko kislino. Produkte smo karakterizirali z FTIR, Ramansko in NMR spektroskopijo. Izvedli smo tudi B3LYP izračune. Konstante senčenja za ^{13}C in ^{1}H atome so bile izračunane z GIAO/B3LYP/6-311G(d,p) pristopom; dobljene rezultate smo tudi analizirali. Teoretične vibracijske parametre smo primerjali z eksperimentalno dobljenimi vrednostmi. Za pripravljene spojine smo na osnovi modela »napovedovanje spektrov aktivnosti za spojine« (*Prediction of Activity Spectra for Substances*, PASSs) tudi ocenili njihov farmakoterapevtski potencial.